



# Maejo International Journal of Energy and Environmental Communication

Journal homepage: <https://ph02.tci-thaijo.org/index.php/MIJEEC>



## ARTICLE

### Decomposition of gas phase benzene under different conditions in atmospheric strong ionization non-thermal plasma

Prince Junior Asilevi\*, Chengwu Yi, Jue Li, Huijuan Wang, and Muhammad Imran Nawaz

School of Environmental and Safety Engineering, Jiangsu University, Zhenjiang 212013, Peoples Republic of China

#### ARTICLE INFO

##### Article history:

Received 26 Jan 2020

Received in revised form

12 April 2020

Accepted 16 May 2020

##### Keywords:

Benzene

Strong ionization DBD,

Decomposition mechanism

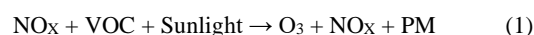
Maxwell equation

#### ABSTRACT

Atmospheric volatile organic compounds (VOCs) from industry and automobiles are posing a serious threat to the environment and human health, and hence efficient control methods are indispensable. This paper presents a laboratory-scale study on the decomposition mechanism for benzene using strong ionization dielectric barrier discharge (DBD) at atmospheric pressure. The specific input energy (SIE), current density, and concentration were studied. The results show that the removal efficiency of benzene increased from 12% to 69% with the increase of SIE from 0.5 to 3.8 kJ/L. The decline in current density by 66.48% and 43.7% for an initial benzene concentration of 300 ppm, was due to increased oxygen content (from 2.4% to 20.9%) and relative humidity (from 18.9% to 90%), respectively, thus electron concentration and consequentially enhancing the removal efficiency over 93%. Further, the beta parameter of the VOC decomposition law decreased from 3.1 kJ/L at 300 ppm to 1.6 kJ/L at 100 ppm. This shows that  $\bullet\text{O}$  and  $\bullet\text{OH}$  radicals are key species for the decomposition of benzene and electron dissociation reactions principally control the process. The highest ozone concentration was detected at 5.5 mg/L when no benzene is present, while the main  $\text{NO}_x$  species ( $\text{NO}$  and  $\text{NO}_2$ ) increased with increasing SIE. The Maxwell-Boltzmann electron energy distribution function was solved using the strong ionization discharge reactor ( $\sim 10$  eV), showing that approximately 84.8% of high-energy electrons possess enough energy to cause the benzene ring cleavage and free radical production. Finally, GCMS and FTIR test results suggested that the byproducts mainly consisted of phenol and substitutions of phenol. The study results show that the strong ionization DBD reactor efficiently removes benzene from polluted air.

## 1. Introduction

Volatile organic compounds (VOCs) are a major environmental menace causing air, water, and soil pollution. In addition, they are responsible for many environmental problems, including atmospheric photochemical reactions leading to ozone formation in the troposphere, ozone depletion in the stratosphere, particulate matter (PM), and the absorption of thermal infrared, thus enhancing global warming (eq. 1).



They are also reported to be carcinogenic, teratogenic and mutagenic, along with other harmful human health effects. The abatement of VOCs has thus become a subject of great worry and intense research for both scientists and engineers in the last few decades. VOCs are emitted from a variety of sources including

\* Corresponding author.

E-mail address: [ev\\_asilevi@yahoo.com](mailto:ev_asilevi@yahoo.com) (Prince Asilevi Junior)

motor vehicles, chemical manufacturing facilities, refineries, factories, consumer and commercial products, and natural (biogenic) sources (mainly trees). Construction technology materials and modern consumer products are important sources of volatile organic compounds (VOCs) in the indoor environment. The emission from materials is usually continuous and may persist for many years in a building structure (Asilevi et al., 2020).

The conventional removal methods include thermal and catalytic combustion, adsorption, membrane separation, biodegradation, and photocatalysis, which have been reported to show relatively low removal efficiency, especially for low VOC concentrations. Meanwhile, the emergence of strict regulations on VOC emission levels poses the mandate to employ precision and accuracy in the decomposition of these pollutants. Reactor efficiency, mechanism, and reactions are among the key issues (Jarraya et al., 2010).

Non-thermal plasma (NTP) technology, has received much attention as a promising technology adaptable to room temperature and atmospheric pressure. It has been shown to be highly efficient, energy saving, and environmentally friendly for the removal of VOCs. Collisions between high energetic electrons and  $O_2/H_2O$  components of polluted air generate active species such as  $\bullet O$  and  $\bullet OH$  which react with pollutants. Notwithstanding, a few setbacks include low energy efficiency, inferior mineralization efficiency and the formation of harmful discharge byproducts such as ozone ( $O_3$ ) and  $NO_x$  ( $NO$  and  $NO_2$ ) (Asilevi et al., 2020; Zhu et al., 2008; Kim et al., 2008).

Dielectric barrier discharge (DBD) is a good source of NTP at atmospheric pressure, and has low cost plasma in air pollution control. It has been shown to be particularly efficient in removing very low concentrations of VOCs and odorous compounds, and has the advantage of energy saving and no production of dioxin. In addition, strong ionization DBD has become doubly attractive owing to its relatively higher average kinetic energy of impact electrons ( $\sim 10$  eV) over that of ordinary DBD systems with impact electron energy of  $\sim 5.0$  eV (Holzer et al., 2002; Hongxiang et al., 2010).

Karatum and Deshusses (2016) studied the removal efficiency of some common VOCs using DBD reactor under similar experimental conditions (i.e. gas residence time of 0.016 s and initial concentration of 95–100 ppm). The following removal efficiencies were reported: methyl ethyl ketone (50%), benzene (58%), toluene (74%), 3-pentanone (76%), methyl tert-butyl ether (80%), ethylbenzene (81%), and n-hexane (90%). Apparently, different VOCs have different removal efficiencies. Mok and Nam (2002) have noted that plasma generated radicals are the main active species responsible for the decomposition of VOCs in the DBD. Thus oxygen and water vapor may play key roles in the abatement process, since they are the main sources of  $\bullet O$  and  $\bullet OH$  radicals in the plasma system. Xu et al., (2014) have studied the effect of CuO/AC catalyst with the pulsed corona discharge in enhancing the removal efficiency of benzene. Recently, Liang et al., (2013) also used a ferroelectric catalyst with the DBD to remove toluene. The study underscored the significant role of ozone produced in the plasma in the degradation process, with

principal emphasis on catalyst effect. Zhu et al. (2008) combined the DBD and titanium dioxide photocatalyst in the abatement of benzene from industry polluted air. Most researchers have focused on improving reactor function largely by the synergistic effect of catalytic metals and photocatalytic technology, although most catalysts have been reported to show poisoning effects. Again, the effect of electrical characteristics of the DBD device which drives the decomposition process remains largely nascent in most literature (Mao et al., 2018; Guo et al., 2015; Wu et al., 2017). . The aim of this paper is to study the feasibility benzene degradation by a homemade strong ionization DBD. We focused on the mechanism and reactor discharge conditions required for the degradation. Benzene is an aromatic and highly volatile carcinogenic VOC which benumbs the central nervous system and has detrimental effects on human health. In addition, it is reportedly the most predominant VOC of the total emissions of hazardous gases from vehicles using conventional gasoline, representing the main source of benzene pollution (Halliday et al., 2016). Furthermore, the role of initial benzene concentration, relative humidity, and input energy density was studied, along with ozone and  $NO_x$  byproducts were explored.

## 2. Materials and Methods

Fig. 1 is a schematic representation of the whole experimental setup employed in this research.

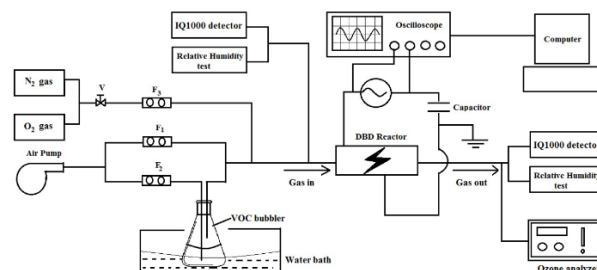


**Fig. 1** Schematic of the experimental set-up. V is control valve, while F<sub>1</sub>, F<sub>2</sub>, and F<sub>3</sub> are the gas mass flow rate meters calibrated in L/min.

The main parts are: (1) the gas flow system comprising the air pump, nitrogen and oxygen gas supply tanks under flow control, (2) the reactor system comprising of the DBD reactor, high voltage AC supply, and (3) the analytic system comprising of the IQ1000 benzene concentration detector, humidity meter, oscilloscope and computer. The volume of the strong ionization discharge reactor is 19 cm<sup>3</sup>, and the supply voltage frequency is set at 5.883 kHz. The experimental conditions are summarized in Table 1.

**Table 1** Experimental measurement conditions.

Parameter	Value
Supply frequency	5.883 kHz
Reactor volume	19 cm <sup>3</sup>

Benzene concentration	100–400 ppm
Nitrogen flow rate	0.0–1.0 L/min
Relative humidity	15.5–80 %
Voltage	1.0–3.0 kV

### 2.1 The gas flow system

Nitrogen gas under valve control along with air is bubbled through the diluted benzene solution prepared at some suitable concentration consistent with the detector limit, placed in a water bath at room temperature. The gaseous mixture then inlets the discharge reactor under varying humidity conditions by changing the temperature of the water bath. The valve controls the amount of nitrogen gas passing into the reactor. The gas flow rate meters  $F_1$ ,  $F_2$ , and  $F_3$  measure the rates at which the gases flow through the experimental system in L/min.

### 2.2 The reactor system

Fig. 2 is a schematic view of the strong ionization DBD reactor system used in the experiment. The reactor is a rectangular box, 227 mm  $\times$  145 mm  $\times$  22 mm in dimension. The sintered metallic silver grounding electrodes are 100 mm  $\times$  190 mm, housing a double 1 mm narrow gas gap serving as the discharge reaction chamber. The housing structure is designed to provide a heat sink along with an electric fan fixed close to the reactor for cooling during discharge operation. Across the reactor is a high voltage alternating current power supply to provide the discharge energy.

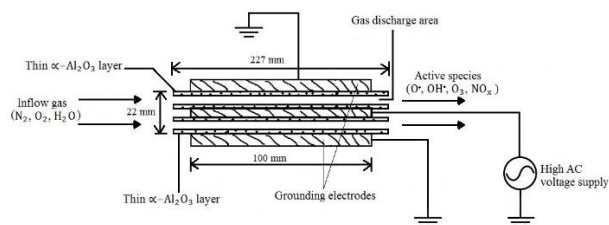


**Fig. 2** Schematic representation of the strong ionization DBD reactor.

### 2.3 The analysis system

The inlet gas is first analyzed before it enters the ionization reactor chamber. This is done using the Model IQ-1000 (International Sensor Technology, California), which is a portable universal gas detector. The instrument is equipped with the Mega-Gas Sensor, a solid state sensor designed to detect over 100 toxic and combustible gases. The calibration is simple and automated with no manual adjustments necessary. The IQ-1000 stores the setup and calibration data for each gas in memory. When a gas is selected from the IQ-1000's menu, the IQ-1000 automatically uses the data to configure itself properly for the gas selected, allowing the unit to provide an accurate reading of the gas concentration.

Power is provided by 6 'D' size alkaline or nickel cadmium batteries. Finally, the recorded data is displayed on a large backlit LCD screen and then transferred to the computer via an RS-232 port for further analysis. A similar test is repeated for the outlet gas to determine the concentration of the remnant benzene pollutant in parts per million (ppm). The concentration of ozone produced by the DBD at the outlet is detected and measured by the ozone concentration analyser (CL-7685, B&C electzanice, Italy).  $\text{NO}_x$  concentration is measured by the NOVA5003-S gas analyser (tenova, USA). The instrument employs electrochemical principle to measure the concentration of NO and  $\text{NO}_2$ . The range of NO is 0–5000 ppm, while  $\text{NO}_2$  has a range of 0–800 ppm and a resolution of 1 ppm.

A high voltage-time 500 MHz digital oscilloscope (WaveJet 354A) is connected across the high voltage supply to obtain the voltage and charge waveforms. This is done by connecting the high voltage probe (Tektronix, P6015A). The discharge current density is measured with a current probe (Tektronix, TCP303) and the root mean square (RMS) value is analyzed.

The organic byproducts during the decomposition of benzene were determined by Agilent 6890 gas Chromatography (GC) combined with a 5975 mass spectrometer (MS) (Aligent Technologies, CA, USA), fitted with an on board flame ionization detector (FID) and helium carrier gas (1 mL/min, constant flow). The sample solution was prepared by dissolving the outlet gas in ethanol, and injected into the instrument gas stream using the splitless injection mode. An Agilent DB-5MS (30 m  $\times$  0.25 mm  $\times$  0.25  $\mu\text{m}$ ) capillary column was used for the separation. The column separation tube was set at 170  $^\circ\text{C}$  column temperature, 250  $^\circ\text{C}$  injection temperature, and 280  $^\circ\text{C}$  detection temperature. The injection volume of the injector is 10  $\mu\text{L}$ . Initial temperature was set at 40  $^\circ\text{C}$  for 3 min, with heating rate of 10  $^\circ\text{C}/\text{min}$  up to 100  $^\circ\text{C}$ , again, 5  $^\circ\text{C}$  per minute up to 200  $^\circ\text{C}$ , then 10  $^\circ\text{C}/\text{min}$  up to 300  $^\circ\text{C}$ . Total time for the analysis was 38.98 min. Fourier transform infrared spectrum (FT-IR) was taken using KBr pellet method with the Nicolet Nexus 470 FT-IR spectrophotometer from Thermo Electron Corporation.

The input charge,  $Q$ , is obtained by measuring the capacitor voltage in series with the ground electrode of the reactor in order to calculate the input power using the  $V$ - $Q$  Lissajous diagram from the oscilloscope. The entire signal data is processed by the computer connected to the oscilloscope. All calculations and graphical representations were performed on the MATLAB Toolbox Release 2012b, The MathWorks, Inc., Natick, Massachusetts, United States.

### 2.4 Electrical measurements and calculations

VOC decomposition is principally governed by the electricity within the plasma system. It is therefore of key relevance to quantify the energy released into the system. Thus the following calculations were performed:

**Specific input energy (SIE):** This is the energy used within the reactor for the decomposition process by a unit volume of

polluted gas (Wu et al., 2017). It is calculated as:

$$\text{SIE} = 60P/F \quad (2)$$

where  $P$  is the high voltage input power and  $F$  is the gas flow speed measured in L/ min.

**Degree of removal ( $C_{out}/C_{in}$ ):** This is the ratio of final VOC concentration after degradation to initial VOC concentration. For a particular VOC pollutant, the removal degree is dependent on the SIE and an input energy parameter called  $\beta$  (beta-parameter) according to eq. 2.

$$C_{out} = C_{in} \exp(\text{SIE}/\beta) \quad (3)$$

where  $C_{in}$  and  $C_{out}$  are the initial and output benzene concentrations, and  $\beta$  is the specific energy constant. The degree of removal reduces as more pollutant is removed and hence the removal efficiency can be obtained as:  $1 - (C_{out}/C_{in})$  (Rosocha, 2005).

**Discharge power (P):** It is the average electrical power in watts (W) deposited into and consumed by the plasma ionization reactor chamber. This is needed to calculate the SIE and to characterize the decomposition energy consumption. This paper follows the  $Q-V$  Lissajous curve method for calculating discharge power, first reported by Manley (1943), and recently shown by a host of researchers to give viable results for energy studies in DBD plasma reactor studies (Kriegseis et al., 2011). It is given as:

$$P = \frac{1}{T} \int_0^T V_r(t) \cdot C_m \frac{dV_m(t)}{dt} dt = \frac{1}{T} \int V_r C_m dV_m = \frac{1}{T} \oint V_r dQ_m \quad (4)$$

where  $T$  is the AC cycle period,  $V_r$  is the high voltage across the reactor,  $C_m$  is the capacitance of the series capacitor also called monitor capacitor. A large capacitance must be chosen relative to the reactor capacitance in order to ensure a very small voltage ( $V_m$ ) across it.  $Q_m$  is the charge on the capacitor. In the experiment, a 4.7  $\mu\text{F}$  capacitor is chosen (see figure 1). The small voltage drop ( $V_m$ ) across the series capacitor is measured with the MASTECH MY-65 digital multimeter, which is then entered into a MATLAB code to compute the charge,  $Q_m$ .

A graph of  $Q_m$  against  $V_r$  displayed on the oscilloscope is usually a parallelogram, called the Lissajous curve, whose area is the energy deposited within the reactor. Thus, equation (3) can finally be written as:

$$P = f \times A \quad (5)$$

where  $f$  is the high voltage AC frequency in Hertz and  $A$  is the Lissajous area. The electric signals are measured by the digital oscilloscope.

### 3 Results and Discussion

#### 3.1 Energy characteristics of discharge reactor

In order to discuss decomposition of benzene, the energy

deposited within the DBD reactor is an indispensable parameter for efficient function. This paper uses the  $Q-V$  Lissajous method to obtain power deposited into the DBD. The Lissajous curve has a parallelogram shape whose area equals the energy deposited (Kriegseis et al., 2011).

The typical voltage and current waveforms of the strong ionization DBD displayed on the oscilloscope are shown in fig. 3. The applied voltage amplitude is 3.5 kV, with the corresponding current waveform showing several short peaks, indicating micro discharge activity in the DBD plasma.

The decomposition efficiency of benzene was enhanced with increasing oxygen concentration by volume and increasing water vapor (RH). This indicates that the benzene was effectively decomposed by the production of the active species in the strong ionization DBD reactor. The amount of energy deposited into the reactor, SIE in J/L is also correlated with the removal efficiency.

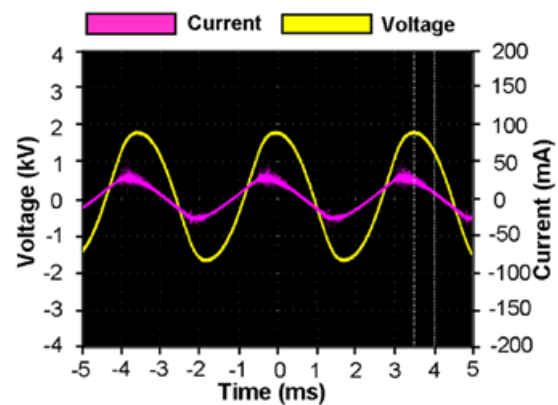


**Fig. 3** Typical voltage and current waveforms of strong ionization dielectric barrier discharge in air, displayed on the oscilloscope.

Fig. 4 shows the removal efficiency under different relative humidity (RH) conditions in the strong ionization DBD for 300 ppm of benzene (15.5%, 30.9%, 68.2%, and 80%). Efficiency of removal at 0.5 kJ/L is 45.5%, 59.1%, 70.4%, and 73.7% respectively, and for a relatively higher SIE of 3.5 kJ/L it is 70.4%, 84.9%, 93.9%, and 96.2% respectively. Apparently, the evolution of removal efficiency is enhanced by appreciably more humid air notwithstanding the insignificance at closely higher RH. Future study will investigate temperature and ozone effects, since temperature relates linearly with molecular energy and ozone is reportedly an important gaseous product of air plasma ionization (Khan and Ghoshal, 2000). When the oxygen volume concentration increased from 3.7% to 8.7% the decomposition efficiency is enhanced almost by 57.68%.

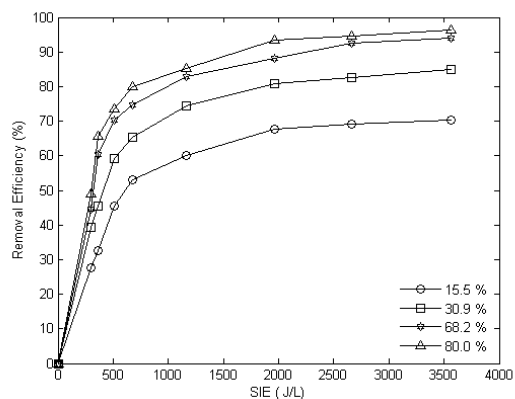


**Fig. 4** Impact of SIE on removal efficiency with respect to RH (15.5%, 30.9%, 68.2%, and 80%) for 300 ppm initial benzene concentration in air.

### 3.2 Effect of initial Benzene concentration

Fig. 5 shows the impact of initial benzene concentration on pollutant removal with respect to oxygen concentration. The initial concentration is varied in the range of 50–390 ppm with a total gas flow rate of 10 L/min and supply voltage of 2.8 kV. It is apparent that the efficient removal of benzene pollutant is significantly dependent on the initial concentration of benzene as well as the amount of oxygen content in the flow air. This is shown by the decreasing trend in the removal efficiency, as the initial concentration increases. For example, the removal efficiency is 88% at initial concentration of 50 ppm but decreases to 70% as initial concentration increases to 350 ppm, for ambient air conditions. For a given processed stream, the amount of reactive species, high-energy electrons and active species generated by plasma could be same at a certain operating condition. Increasing the inlet concentration of benzene will increase the number of benzene molecules flowing into the reactor. That is to say, each benzene molecule shares less active species and electrons, leading to a reduction of effective benzene removal efficiency (Khan and Ghoshal, 2000).

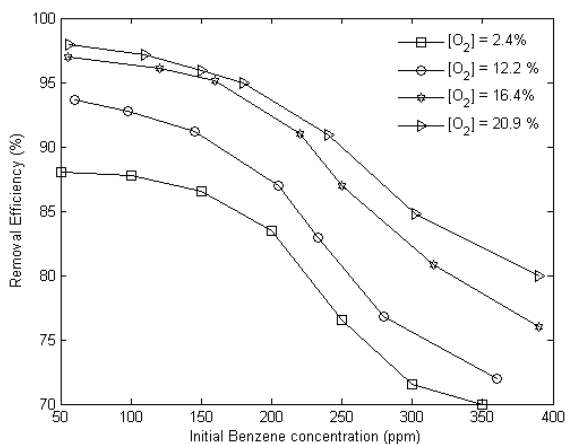


**Fig. 5.** Impact of initial benzene concentration on benzene

decomposition efficiency for different oxygen content conditions, at 2.8 kV and a total air flow rate of 4 L/min.

### 3.3 Production of ozone ( $O_3$ )

Fig. 6 shows the variation of ozone produced by the strong ionization DBD with SIE under different initial concentrations of the benzene pollutant. It is noticed that ozone production is highest (5.5 mg/L) at SIE of 3.56 kJ/L when no benzene is present and lower (0.8 mg/L) at SIE of 4.16 kJ/L when benzene concentration is 100 ppm. Apparently, the presence of benzene pollutant suppressed the production of ozone. This is consistent with the observation of Jiang et al., 2013 and Karatum and Deshusses (2016), and is reportedly the result of ozone consumption during the oxidative degradation of VOCs in the DBD. Another significant observation is the sharp decline of ozone production after a maximum is reached for all three cases. This has been attributed to the rising temperature and increased electron density in the discharge reactor as SIE increases, resulting in the quick breakdown of ozone (Liang et al., 2013; Yao et al., 2015).

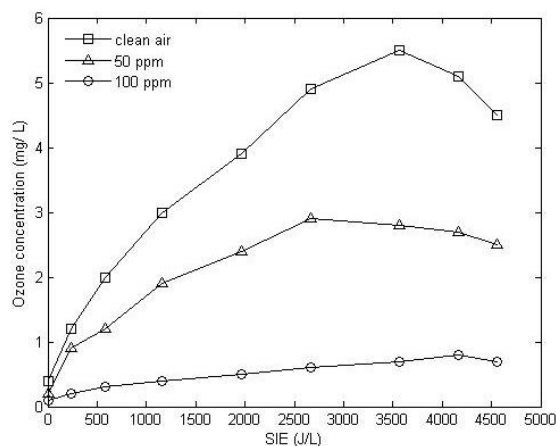


**Fig. 6** Ozone formation under varying SIE for oxygenated clean air, 50 ppm, and 100 ppm of benzene in air and oxygen gas, and 4 L/min flow rate.

### 3.4 Production of $NO_x$

$NO_x$  is an important byproduct of DBD reactor, predominantly resulting from nitrogen in the air used as carrier gas (Xu et al., 2014). Fig. 7 shows the concentration of the main  $NO_x$  species (NO and  $NO_2$ ), detected at ambient temperature (27 °C) and atmospheric pressure. For the SIE range of 239.2–4162.1 J/L, the concentration range of NO and  $NO_2$  are 3.58–10.92 mg/m<sup>3</sup> and 19.22–40.59 mg/m<sup>3</sup> respectively. It is clear that, the concentrations of the two main  $NO_x$  species (NO and  $NO_2$ ) increases with increasing SIE, while the concentration range of NO is lower than  $NO_2$ . This is attributed to the presence of ozone and other active species ( $\bullet O$  and  $\bullet OH$ ) generated by the discharge reactor, which quickly oxidizes NO. Yu-fang et al., (2006) have shown a series of possible reactions leading to the formation and oxidation of  $NO_x$  species during a DBD – catalyst process.

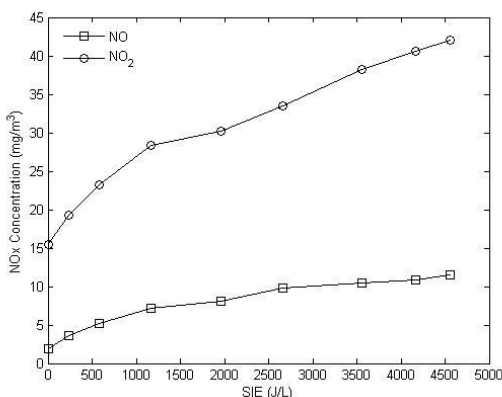


**Fig. 7** NO<sub>x</sub> formation under varying SIE at 100 ppm benzene and 4 L/ min flow rate in air.

### 3.6 Decomposition mechanism of benzene

#### 3.6.1 Benzene cleavage and electron energy

In order to understand the breakdown of benzene in our strong ionization plasma, it is important to account for the role of energetic electrons within the ionization discharge chamber, hence the amount of benzene consumed and byproduct formation. According to Ye et al. (2008) the energy of electrons available within the reactor chamber widely varies and thus follows a Maxwellian distribution function shown in eq. 6 below:

$$E(a) = \int_a^{+\infty} 0.185\varepsilon^{1/2} e^{-0.3\varepsilon} d\varepsilon \quad (6)$$

In the above equation,  $E(a)$  is the percent amount of electrons possessing the minimum energy required for bond cleavage. The term  $\varepsilon$  is the average energy of electrons in the plasma ionization reactor.

Benzene is a very stable hydrocarbon composed of six carbon atoms joined in a ring with one hydrogen atom attached to each. Cleavage of the benzene ring requires about 5.4 eV. Since the average energy of electrons in the strong ionization discharge reactor is ~10 eV, by solving eq. 6, we obtain approximately 84.8% of electrons possessing the minimum energy required to cause cleavage in benzene. This means that more than half of electron – benzene collision can effectively result in a complete breakdown producing CO<sub>2</sub> and H<sub>2</sub>O directly. Meanwhile, not all energetic electrons will proceed to initial benzene cleavage, some accounting the production of •O and •OH radicals. This may be responsible for the appreciably high decomposition efficiencies reaching 90% and beyond realized in this experiment. Hongxiang et al. (2010) have shown that removal efficiencies in strong ionisation discharge can exceed 93% (almost complete VOC abatement).

#### 3.6.2 Benzene cleavage byproducts

Fig. 8 shows the GC-MS display of the gaseous byproducts at

the outlet resulting from the decomposition of benzene by the strong ionization DBD. It is apparent that, some organic compounds resulting from the decomposition of benzene have been detected. The high electron energy (~10 eV) and the high free radical reactivity in the strong ionization plasma reactor, affords high removal efficiency. Fig. 8 (a) shows the preliminary chromatographic result for the outlet gas at 300 ppm benzene concentration before the discharge process. Two large peaks representing ethanol and benzene at peak intensities of 2855 and 7195 respectively, were detected. This is expected, since the gaseous benzene in the synthetic polluted air was collected in ethanol.

Fig.8 (b) displays the chromatogram for the outlet gas at 300 ppm benzene and 2.5 kV. After the collision of high energy electrons with benzene to form phenyl (C<sub>6</sub>H<sub>5</sub>) radical, a series of addition and substitution reactions continue with •O and •OH radicals, along with NO<sub>2</sub> (formed possibly by equation (10)) leading to the formation of 4-nitro-phenol (C<sub>6</sub>H<sub>5</sub>NO<sub>3</sub>), hydroquinone, and phenol (C<sub>6</sub>H<sub>5</sub>OH), at peak intensities of 1750, 1500, and 1389 respectively. Some aliphatic compounds such as Acetic acid, Propenoic acid, and Butanal were also detected between 3 and 4 min along with other peaks such as Hydro-pyrimidine and 4-Phenoxy-phenol. Some other fine peaks are also shown in the chromatogram, but their respective spectral resolutions are very insignificant. High energy electrons may further attack these aromatic compounds, leading to ring cleavage. These organic compounds are similar with the results of other researchers using low voltage DBD operation (Liang et al., 2015; Wang et al., 2017; Jiang et al., 2013; Boucher and Katz, 1967).. The implication is that, the decomposition of benzene in the strong ionization DBD with the •O and •OH radicals, is an environmentally clean technology.

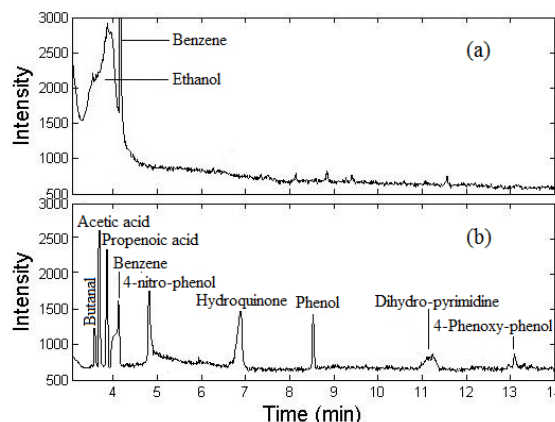


**Fig. 8** GC-MS diagram of organic byproducts in the outlet gas at ambient temperature and 300 ppm initial concentration: (a) inlet gas and (b) outlet gas after plasma treatment.

Fig. 9 shows the emission spectra analysis of the byproducts of benzene decomposition using the FTIR (Fourier Transform Infrared Spectrum) for 300 ppm benzene concentration. The spectrum shows C=C stretching frequency around 1500 cm<sup>-1</sup> in the fingerprint region. A sharp stretch at 2500 cm<sup>-1</sup> is indicative of a C-C peak. This peak could also represent the presence of CO<sub>2</sub>.

Present in the IR spectrum is a weak broad band at  $3300\text{ cm}^{-1}$  signifying the presence of  $-\text{OH}$ . Another sharp and strong peak in the functional group region was observed at  $3700\text{ cm}^{-1}$ . This further shows the presence of  $-\text{OH}$  (Xu et al., 2014; Boucher and Katz, 1967).

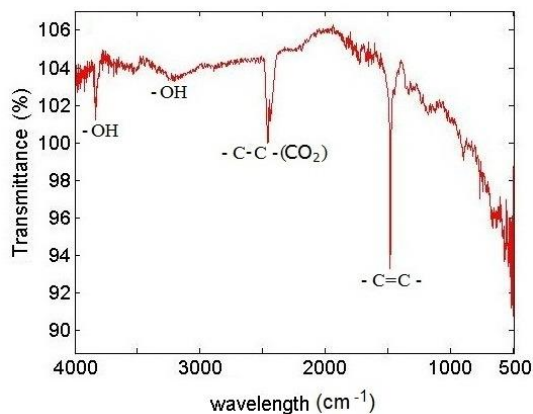


**Fig. 9** FTIR spectrum of the products from decomposition of benzene in strong ionization DBD at ambient temperature, 300 ppm initial concentration, 1.5 kV, and 4 L/ min flow rate in air.

#### 4. Conclusion

This study has achieved a good working knowledge of the mechanism and reactor discharge conditions necessary for the efficient removal of benzene using the strong ionization dielectric barrier discharge reactor at atmospheric pressure. In the experimental, the current probe (Tektronix, TCP2020) connected to the high voltage-time 500 MHz Digital Oscilloscope (WaveJet 354A) was used to monitor the current density in the reactor, when the oxygen content and water vapor is changing.  $\sim 35.5\%$  increase in oxygen content and relative humidity (from 18.9% to 84.1%) reduced the current density by 66.48% and 43.7% respectively. This is accounted for as the result of electron consumption in the breakdown of air molecules such as  $\text{O}_2$ ,  $\text{N}_2$  and  $\text{H}_2\text{O}$  leading to the formation of free active radicals such as  $\bullet\text{O}$  and  $\bullet\text{OH}$ . Concurrently, the removal efficiency of the benzene is observed to increase. It is thus apparent that the  $\bullet\text{O}$  and  $\bullet\text{OH}$  radicals must be key factors controlling the overall breakdown of benzene in the plasma reactor. Meanwhile, the Maxwell-Boltzmann electron energy distribution function also showed that approximately 84.8% of the high energy electrons possess enough energy to cause benzene ring cleavage and free radical production, fitly accounting for the high removal efficiencies realized. Further, the GCMS and FTIR test results revealed that the main decomposition byproducts were 4-nitrophenol ( $\text{C}_6\text{H}_5\text{NO}_3$ ), hydroquinone, and phenol. In the overall, benzene removal from polluted air can be appreciably attained at high efficiencies using the strong ionization DBD other than the low electron energy type technology.

#### Declaration of competing interest

The authors declare that they have no known competing

financial interests or personal relationships that could have appeared to influence the work reported in this paper.

#### Acknowledgments

This work is supported by the Zhenjiang City Key R&D Project for Social Development (SH2017056).

#### References

- Asilevi, P. J., Yi, C. W., Li, J., Nawaz, M. I., Wang, H. J., Yin, L., & Junli, Z. 2020. Decomposition of formaldehyde in strong ionization non-thermal plasma at atmospheric pressure. *International Journal of Environmental Science and Technology*, 17(2), 765-776.
- Boucher, L. J., & Katz, J. J. 1967. The infrared spectra of Metalloporphyrins ( $4000\text{-}160\text{ cm}^{-1}$ ). *Journal of the American Chemical Society*, 89(6), 1340-1345.
- Guo, Y., Liao, X., Fu, M., Huang, H., & Ye, D. 2015. Toluene decomposition performance and  $\text{NO}_x$  by-product formation during DBD-catalyst process. *Journal of Environmental Sciences*, 28, 187-194.
- Halliday, H. S., Thompson, A. M., Wisthaler, A., Blake, D. R., Hornbrook, R. S., Mikoviny, T., ... & Hills, A. J. 2016. Atmospheric benzene observations from oil and gas production in the Denver - Julesburg Basin in July and August 2014. *Journal of Geophysical Research: Atmospheres*, 121(18), 11-055.
- Holzer, F., Roland, U., & Kopinke, F. D. 2002. Combination of non-thermal plasma and heterogeneous catalysis for oxidation of volatile organic compounds: Part 1. Accessibility of the intra-particle volume. *Applied Catalysis B: Environmental*, 38(3), 163-181.
- Hongxiang, O., Chengwu, Y., Wenming, Q., Songmei, W., Qianqian, L., Jing, C., & Li, M. (2010, June). Study on formaldehyde degradation using strong ionization discharge. In 2010 international conference on mechanic automation and control engineering (pp. 2094-2097). IEEE.
- Jarraya, I., Fourmentin, S., Benzina, M., & Bouaziz, S. 2010. VOC adsorption on raw and modified clay materials. *Chemical Geology*, 275(1-2), 1-8.
- Jiang, N., Lu, N., Shang, K., Li, J., & Wu, Y. 2013. Effects of electrode geometry on the performance of dielectric barrier/packed-bed discharge plasmas in benzene degradation. *Journal of hazardous materials*, 262, 387-393.
- Karatun, O., & Deshusses, M. A. 2016. A comparative study of dilute VOCs treatment in a non-thermal plasma reactor. *Chemical Engineering Journal*, 294, 308-315.
- Kriegseis, J., Möller, B., Grundmann, S., & Tropea, C. 2011. Capacitance and power consumption quantification of dielectric barrier discharge (DBD) plasma actuators. *Journal of Electrostatics*, 69(4), 302-312.
- Khan, F. I., & Ghoshal, A. K. 2000. Removal of volatile organic compounds from polluted air. *Journal of loss prevention in the process industries*, 13(6), 527-545.
- Kim, H. H., Ogata, A., & Futamura, S. 2008. Oxygen partial pressure-dependent behavior of various catalysts for the total oxidation of VOCs using cycled system of adsorption and oxygen plasma. *Applied Catalysis B: Environmental*, 79(4), 356

-367.

- Liang, W. J., Ma, L., Liu, H., & Li, J. 2013. Toluene degradation by non-thermal plasma combined with a ferroelectric catalyst. *Chemosphere*, 92(10), 1390-1395.
- Manley, T. C. 1943. The electric characteristics of the ozonator discharge. *Transactions of the electrochemical society*, 84(1), 83.
- Mao, L., Chen, Z., Wu, X., Tang, X., Yao, S., Zhang, X., ... & Nozaki, T. 2018. Plasma-catalyst hybrid reactor with CeO<sub>2</sub>/γ-Al<sub>2</sub>O<sub>3</sub> for benzene decomposition with synergetic effect and nano particle by-product reduction. *Journal of Hazardous Materials* 347, 150-159.
- Mok, Y. S., & Nam, I. S. 2002. Modeling of pulsed corona discharge process for the removal of nitric oxide and sulfur dioxide. *Chemical Engineering Journal*, 85(1), 87-97.
- Rosocha, L. A. 2005. Nonthermal plasma applications to the environment: gaseous electronics and power conditioning. *IEEE transactions on plasma science*, 33(1), 129-137.
- Wang, B., Chi, C., Xu, M., Wang, C., & Meng, D. (2017). Plasma - catalytic removal of toluene over CeO<sub>2</sub>-MnO<sub>x</sub> catalysts in an atmosphere dielectric barrier discharge. *Chemical Engineering Journal*, 322, 679-692.
- Wu, A., Li, X., Yan, J., Yang, J., Du, C., Zhu, F., & Qian, J. 2017. Co-generation of hydrogen and carbon aerosol from coalbed methane surrogate using rotating gliding arc plasma. *Applied Energy*, 195, 67-79.
- Xu, N., Fu, W., He, C., Cao, L., Liu, X., Zhao, J., & Pan, H. 2014. Benzene removal using non-thermal plasma with CuO/AC catalyst: reaction condition optimization and decomposition mechanism. *Plasma Chemistry and Plasma Processing*, 34(6), 1387-1402.
- Yao, S., Wu, Z., Han, J., Tang, X., Jiang, B., Lu, H., ... & Kodama, S. (2015). Study of ozone generation in an atmospheric dielectric barrier discharge reactor. *Journal of Electrostatics*, 75, 35-42.
- Ye, Z., Zhang, Y., Li, P., Yang, L., Zhang, R., & Hou, H. 2008. Feasibility of destruction of gaseous benzene with dielectric barrier discharge. *Journal of Hazardous materials*, 156(1-3), 356-364.
- Yu-fang, G., Dai-qi, Y., Ya-feng, T., & Ke-fu, C. (2006). Humidity effect on toluene decomposition in a wire-plate dielectric barrier discharge reactor. *Plasma chemistry and plasma processing*, 26(3), 237-249.
- Zhu, T., Li, J., Jin, Y. Q., Liang, Y., & Ma, G. 2008. Decomposition of benzene by non-thermal plasma processing: Photocatalyst and ozone effect. *International Journal of Environmental Science & Technology*, 5(3), 375-384.